World Conference on Timber Engineering Oslo 2023

EVALUATION OF VIBRATION PROPERTY OF HIGH-DAMPING TWO-STORY TIMBER STRUCTURE BASED ON RESONANCE CURVE

Yuji Miyazu[1]

ABSTRACT: This paper aims to evaluate the vibration property of a two-story timber structure which has energy dissipation devices to enhance the seismic performance. Oil dampers and friction dampers are considered as the energy dissipation devices in this study. Steady-state response of a two-degree-of-freedom system which has the nonlinear springs with the force-deformation relation of timber structure and the dampers is derived by using the equivalent linearization technique and the sequential quadratic programming. Through the comparison of the resonance curves of the models with/without dampers, it is found that the friction damper reduces the story drift mainly around the first mode while the oil damper works to decrease the story drift both around the first and the second modes.

KEYWORDS: Steady-state response, Resonance curve, Two-story timber structure, High-damping structure

1 INTRODUCTION

Recent years in Japan, energy dissipation devices such as oil dampers and friction dampers are widely used to enhance seismic performance of low-rise timber buildings, especially two-story wooden houses. In some previous researches, the effectiveness of installing energy dissipation devices into timber structures is evaluated numerically through time history seismic response analysis; however, it is also important to investigate the effect of dampers theoretically based on dynamics of structures in order to discuss the vibration property of timber structure that have energy dissipation devices.

The author derived steady-state response of a single-degree-of-freedom system which has a nonlinear spring of ENCL model [1] and viscous and friction elements as energy dissipation devices by using Caughey's equivalent linearization technique [2] in the previous work [3]. In this paper, the steady-state response of a two-degree-of-freedom system are derived in a same manner as the previous method [3] and discuss the vibration property based on resonance curves.

At first, a force-deformation relation model and analysis models used in this study are summarized in Chapter 2. Then, the steady-state response of the two-degree-of-freedom system are derived by using Tajimi's [4] and Caughey's methods [2] in Chapter 3. Finally, the vibration property of a two-story timber structure with energy dissipation devices are discussed in Chapter 4.

2 FORCE-DEFORMATION RELATION OF TIMBER STRUCTURE AND ANALYSIS MODEL

The force-deformation relation of a timber structure is simulated by an extended normalized characteristic loop model (ENCL model) [1] expressed by Eq. (1). $L_1(x)$ and $L_2(x)$ are loading and unloading curves, respectively. The variable x is the deformation normalized by the maximum deformation of the hysteresis loop. A, B, n_1, and n_2 are the parameters which control the shape of the hysteresis loop.

$$\left.\begin{aligned} L_1(x) &= \mp Ax^4 + Bx|x|^{n_1} + (1-B)x \pm A \\ L_2(x) &= \pm Ax^4 + Bx|x|^{n_2} + (1-B)x \mp A \end{aligned}\right\} \quad (1)$$

A represents the force at a y-intercept, and an absorbing energy increases with the increase of the value of A. B controls the slip behaviour of the loop, and a tangent stiffness decreases with the increase of the value of B. n_1 and n_2 control the curvature of the loading and unloading curves, and the curvature increases with the increase of the values of n_1 and n_2.

In this paper, these parameters are adjusted to simulate the force-deformation relation obtained through the static cyclic loading test on the timber beam and column frame combined with plywood panel [5]. Figure 1 shows the force-deformation relation simulated by ENCL model, and its parameters are listed in Table 1. The deformation and the force are expressed by μ and r, and these values are normalized by the deformation and the force at 1/360 rad, respectively.

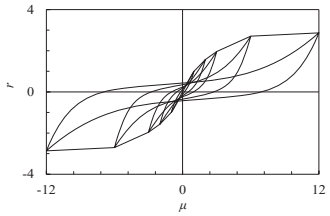

Figure 1: *Force-deformation relation of the timber structure simulated by ENCL model*

[1] Yuji Miyazu, Tokyo University of Science, Japan, miyazu@rs.tus.ac.jp

https://doi.org/10.52202/069179-0272

Table 1: *Parameters of the ENCL model*

Drift angle (rad)	μ	r	A	B	n_1	n_2
0	0	0	0	0	1	1
1/720	0.5	0.5	0	0	1	1
1/360	1	1	0.12	0.3	1	1.6
1/180	2	1.568	0.12	0.54	1	2.4
1/120	3	1.958	0.12	0.66	1.2	2.8
1/60	6	2.704	0.13	0.76	1.9	4.3
1/30	12	2.865	0.15	0.82	2	5.1

Figure 2 illustrates the composition of the analysis models used in this study. The Basic model is the two-degree-of-freedom system which has nonlinear springs with the ENCL model and dashpots representing the inherent structural damping. The VD model has additional dashpots (Dashpot 2) to consider the viscous force added by oil dampers. The FD model has elastic-perfectly plastic springs (EPP springs) which express the stiffness and the friction force added by friction dampers.

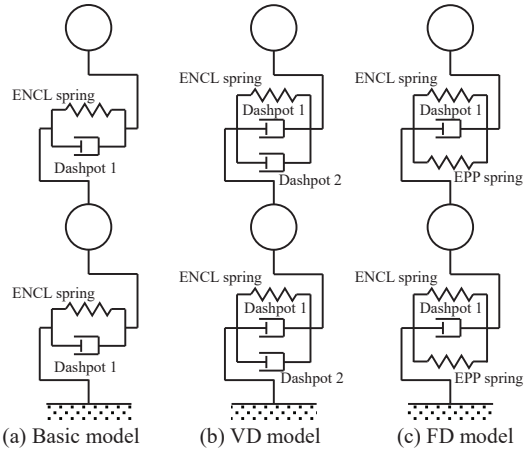

Figure 2: *Composition of analysis models*

3 STEADY-STATE RESPONSE

The equation of motion is formulated as Eq. (2) using story deformation represented by u_1 and u_2 for the first and the second stories, respectively.

$$\left.\begin{aligned} &m_2\left(\ddot{u}_2+\ddot{u}_1\right)+\left(c_2+c_{\mathrm{d}2}\right)\dot{u}_2+k_2Q_2=-m_2\alpha\cos pt \\ &m_2\ddot{u}_2+\left(m_1+m_2\right)\ddot{u}_1+\left(c_1+c_{\mathrm{d}1}\right)\dot{u}_1+k_1Q_1=-\left(m_1+m_2\right)\alpha\cos pt \end{aligned}\right\} \tag{2}$$

where m_i is the mass of ith node, c_i is the viscous damping coefficient of the ith story related to inherent damping of timber structure, $c_{\mathrm{d}i}$ is the viscous damping coefficient added by oil dampers in the ith story, k_i is the stiffness of the ith story, Q_i is the function of restoring force of the ith story, α is the magnitude of an excitation, and p is the circular frequency of the excitation. Here, we approximate the solution of Eq. (2) as follows.

$$u_i=\mu_i\cos\left(pt-\varphi_i\right)\qquad\left(i=1,2\right) \tag{3}$$

The restoring force of ith story is approximated as follows by using Caughey's equivalent linearization technique.

$$k_iQ_i=k_i\left(k_{ei}u_i+c_{ei}\dot{u}_i\right) \tag{4}$$

where

$$k_{ei}=C_i,\quad c_{ei}=-\frac{S_i}{p} \tag{5}$$

C_i and S_i in Eq. (5) are the values defined in the Caughey's equivalent linearization technique, and they are calculated as the summation of the values of ENCL and EPP springs as formulated in Eq. (6).

$$\begin{aligned} C_i&=C_{i\_\mathrm{ENCL}}+C_{i\_\mathrm{EPP}} \\ S_i&=S_{i\_\mathrm{ENCL}}+S_{i\_\mathrm{EPP}} \end{aligned} \tag{6}$$

C_{i_ENCL} and S_{i_ENCL} are calculated by Eq. (7) which was derived in the previous study [3].

$$\begin{aligned} C_{i\_\mathrm{ENCL}}&=\frac{2}{\mu_i\pi}\left[\int_{-\frac{\pi}{2}}^{0}r_iL_1\left(\cos\theta\right)\cos\theta d\theta\right. \\ &\qquad\left.+\int_{0}^{\frac{\pi}{2}}r_iL_2\left(\cos\theta\right)\cos\theta d\theta\right] \\ &=\frac{2r_i}{\mu_i\pi}\left\{\frac{\sqrt{\pi}}{2}\left(\frac{\Gamma\left(\frac{n_1+3}{2}\right)}{\Gamma\left(\frac{n_1+4}{2}\right)}+\frac{\Gamma\left(\frac{n_2+3}{2}\right)}{\Gamma\left(\frac{n_2+4}{2}\right)}\right)B+\frac{\pi}{2}\left(1-B\right)\right\} \\ S_{i\_\mathrm{ENCL}}&=\frac{2}{\mu_i\pi}\left[\int_{-\frac{\pi}{2}}^{0}r_iL_1\left(\cos\theta\right)\sin\theta d\theta\right. \\ &\qquad\left.+\int_{0}^{\frac{\pi}{2}}r_iL_2\left(\cos\theta\right)\sin\theta d\theta\right] \\ &=\frac{2r_i}{\mu_i\pi}\left\{-\frac{8}{5}A+\frac{1}{2}\left(\mathrm{B}\left(1,\frac{n_2+2}{2}\right)-\mathrm{B}\left(1,\frac{n_1+2}{2}\right)\right)B\right\} \end{aligned} \tag{7}$$

C_{i_EPP} and S_{i_EPP} are calculated by Eq. (8) based on the method proposed by Caughey [6].

$$\begin{aligned} C_{i\_\mathrm{EPP}}&=\begin{cases}\dfrac{F_i}{\mu_{yi}\pi}\left(\theta^*-\dfrac{\sin 2\theta^*}{2}\right) & \mu_i>\mu_{yi}\\ \dfrac{F_i}{\mu_{yi}} & \mu_i\le\mu_{yi}\end{cases} \\ S_{i\_\mathrm{EPP}}&=\begin{cases}\dfrac{-F_i}{\mu_{yi}\pi}\sin^2\theta^* & \mu_i>\mu_{yi}\\ 0 & \mu_i\le\mu_{yi}\end{cases} \end{aligned} \tag{8}$$

where $\theta^*=\cos^{-1}\left(1-2\mu_{yi}/\mu_i\right)$, F_i is the ratio of the yield force of the EPP spring to the force of the ENCL model in the ith story at 1/360 rad. μ_{yi} is the yield deformation of the EPP spring in the ith story. By substituting Eqs. (3) and (5) for Eq. (4), and by replacing $pt-\varphi_i$ with θ_i, the restoring force of the ith story is expressed as follows.

$$k_iQ_i=k_i\mu_i\left(C_i\cos\theta_i+S_i\sin\theta_i\right) \tag{9}$$

First, we replace $pt-\varphi_2$ with θ_2 in Eq. (3) to obtain Eq. (3').

https://doi.org/10.52202/069179-0272

$$u_1 = \mu_1 \cos(\theta_2 + \varphi_2 - \varphi_1), \quad u_2 = \mu_2 \cos\theta_2 \tag{3'}$$

By substituting Eqs. (3') and (9) for the upper equation of Eq. (2), we obtain Eq. (2').

$$\begin{aligned} &-p^2 m_2 \{\mu_2 \cos\theta_2 + \mu_1 \cos\theta_2 \cos(\varphi_2 - \varphi_1) - \mu_1 \sin\theta_2 \sin(\varphi_2 - \varphi_1)\} \\ &-(c_2 + c_{d2}) p \mu_2 \sin\theta_2 + k_2 \mu_2 (C_2 \cos\theta_2 + S_2 \sin\theta_2) \\ &= -m_2 \alpha (\cos\theta_2 \cos\varphi_2 - \sin\theta_2 \sin\varphi_2) \end{aligned} \tag{2'}$$

Since Eq. (2') is an identity, we obtain the following relations.

$$\begin{aligned} &-p^2 m_2 \{\mu_2 + \mu_1 \cos(\varphi_2 - \varphi_1)\} \\ &\qquad + k_2 \mu_2 C_2 = -m_2 \alpha \cos\varphi_2 \end{aligned} \tag{10-1}$$

$$\begin{aligned} &p^2 m_2 \mu_1 \sin(\varphi_2 - \varphi_1) - (c_2 + c_{d2}) p \mu_2 \\ &\qquad + k_2 \mu_2 S_2 = -m_2 \alpha \sin\varphi_2 \end{aligned} \tag{10-2}$$

By multiplying $-i$ to Eq. (10-2) and adding it to Eq. (10-1), we obtain Eq. (11).

$$\begin{aligned} &-p^2 \mu_1 e^{-i\varphi_1} \\ &+\left[-p^2 + \frac{c_2 + c_{d2}}{m_2} pi + \frac{k_2}{m_2}(C_2 - iS_2)\right] \mu_2 e^{-i\varphi_2} = -\alpha \end{aligned} \tag{11}$$

Next, we replace $pt - \varphi_1$ with θ_1 in Eq. (3) to obtain Eq. (3'').

$$u_1 = \mu_1 \cos\theta_1, \quad u_2 = \mu_2 \cos(\theta_1 + \varphi_1 - \varphi_2) \tag{3''}$$

By substituting Eqs. (3'') and (9) for the lower equation of Eq. (2), we obtain Eq. (2'').

$$\begin{aligned} &-p^2 m_2 \mu_2 \{\cos\theta_1 \cos(\varphi_1 - \varphi_2) - \sin\theta_1 \sin(\varphi_1 - \varphi_2)\} \\ &-(m_1 + m_2) p^2 \mu_1 \cos\theta_1 - (c_1 + c_{d1}) p \mu_1 \sin\theta_1 \\ &+ k_1 \mu_1 (C_1 \cos\theta_1 + S_1 \sin\theta_1) \\ &= -(m_1 + m_2) \alpha (\cos\theta_1 \cos\varphi_1 - \sin\theta_1 \sin\varphi_1) \end{aligned} \tag{2''}$$

Since Eq. (2'') is also an identity, we obtain the following relations.

$$\begin{aligned} &-p^2 m_2 \mu_2 \cos(\varphi_1 - \varphi_2) - (m_1 + m_2) p^2 \mu_1 \\ &\qquad + k_1 \mu_1 C_1 = -(m_1 + m_2) \alpha \cos\varphi_1 \end{aligned} \tag{12-1}$$

$$\begin{aligned} &p^2 m_2 \mu_2 \sin(\varphi_1 - \varphi_2) - (c_1 + c_{d1}) p \mu_1 \\ &\qquad + k_1 \mu_1 S_1 = (m_1 + m_2) \alpha \sin\varphi_1 \end{aligned} \tag{12-2}$$

By multiplying $-i$ to Eq. (12-2) and adding it to Eq. (12-1), we obtain Eq. (13).

$$\begin{aligned} &\left[-p^2 + \frac{c_1 + c_{d1}}{m_1 + m_2} pi + \frac{k_1}{m_1 + m_2}(C_1 - iS_1)\right] \mu_1 e^{-i\varphi_1} \\ &\qquad - \frac{m_2}{m_1 + m_2} p^2 \mu_2 e^{-i\varphi_2} = -\alpha \end{aligned} \tag{13}$$

Equations (11) and (13) can be written in matrix form in the same manner as Kikuchi et al [7]:

$$\begin{Bmatrix} \mu_1 e^{-i\varphi_1} \\ \mu_2 e^{-i\varphi_2} \end{Bmatrix} = \begin{bmatrix} A_{11} & A_{12} \\ A_{21} & A_{22} \end{bmatrix}^{-1} \begin{Bmatrix} -\alpha \\ -\alpha \end{Bmatrix} \tag{14}$$

where

$$\begin{aligned} A_{11} &= -p^2 \\ A_{12} &= -p^2 + \frac{c_2 + c_{d2}}{m_2} pi + \frac{k_2}{m_2}(C_2 - iS_2) \\ A_{21} &= -p^2 + \frac{c_1 + c_{d1}}{m_1 + m_2} pi + \frac{k_1}{m_1 + m_2}(C_1 - iS_1) \\ A_{22} &= -\frac{m_2}{m_1 + m_2} p^2 \end{aligned}$$

The story drift μ_i is expressed by Eq. (15).

$$\begin{Bmatrix} \mu_1 \\ \mu_2 \end{Bmatrix} = \frac{\alpha}{|A_{11}A_{22} - A_{12}A_{21}|} \begin{Bmatrix} |A_{22} - A_{12}| \\ |A_{11} - A_{21}| \end{Bmatrix} \tag{15}$$

Equation 15 cannot be solved explicitly since A_{12} and A_{21} are also the function of μ_i; therefore, the sequential quadratic programming (SQP) was used to solve the optimization problem formulated by Eq. (16).

$$\begin{aligned} \text{Minimize} \quad & f = \left|\mu_1 - \frac{|A_{22} - A_{12}|}{|A_{11}A_{22} - A_{12}A_{21}|}\alpha\right| \\ & + \left|\mu_2 - \frac{|A_{11} - A_{21}|}{|A_{11}A_{22} - A_{12}A_{21}|}\alpha\right| \\ \text{subject to} \quad & 0 \le \mu_i \le 12, \quad i = 1, 2 \end{aligned} \tag{16}$$

4 RESONANCE CURVE

4.1 PARAMETER OF ANALYSIS MODEL

The detail of the analysis models used here is listed on Table 2. The parameters of c_{d1} and c_{d2} are the viscous damping coefficients added by oil dampers in the first and the second story, respectively. In all the models, m_1 and m_2 are unity, and the values of c_1 and c_2 are decided to let the model have the inherent structural damping of 1% to the initial stiffness of the ENCL springs.

The M1 is the basic model in this study. The mode shape of the first mode in the elastic region of the M1 is an inverted triangle, which is expected to have an almost uniform deformation along the height of the model under ground excitation. The k_1 and k_2 of the M1_R_1.25, 1.5 and 2 are 1.25, 1.5 and 2 times larger than those of the M1, respectively. The M1_V_3%, 5% and 10% has dashpots representing oil dampers in all the stories, and the viscous damping coefficients of the dashpots are decided to have the damping ratio of 3%, 5% and 10% to the initial stiffness of the ENCL springs, respectively. The M1_F_0.1, 0.3 and 1 contain EPP springs representing friction dampers in all the stories. The number put after F_ means the value of F_i which is the ratio of the yield force of the EPP spring to the force of the ENCL model in the ith story at 1/360 rad as mentioned in Chapter 3. The yield deformation of the EPP spring is 1/360 rad in all the M1_F models.

The M2 is another basic model in this study. The stiffness k_1 and k_2 of the M2 are unity, so the story drift in the first story is supposed to become larger than that of the second story under ground excitation. This type of two-story wooden houses is very common in Japan because most houses have many rooms, i.e. many walls, in the second story. For the M2 model, strengthening only in the first

Table 2: *Parameters of analysis models*

Name	Model type	m_1	m_2	k_1	k_2	c_{d1}	c_{d2}	F_1	F_2
M1	Basic model	1	1	1	0.667	0	0	0	0
M2	Basic model	1	1	1	1	0	0	0	0
M1_R_1.25	Basic model	1	1	1.25	0.833	0	0	0	0
M1_R_1.5	Basic model	1	1	1.5	1	0	0	0	0
M1_R_2	Basic model	1	1	2	1.333	0	0	0	0
M1_V_3%	VD model	1	1	1	0.667	0.104	0.069	0	0
M1_V_5%	VD model	1	1	1	0.667	0.173	0.115	0	0
M1_V_10%	VD model	1	1	1	0.667	0.346	0.231	0	0
M1_F_0.1	FD model	1	1	1	0.667	0	0	0.1	0.067
M1_F_0.3	FD model	1	1	1	0.667	0	0	0.3	0.2
M1_F_1	FD model	1	1	1	0.667	0	0	1	0.667
M2_R_1.25	Basic model	1	1	1.25	1	0	0	0	0
M2_R_1.5	Basic model	1	1	1.5	1	0	0	0	0
M2_R_2	Basic model	1	1	2	1	0	0	0	0
M2_V_3%	VD model	1	1	1	1	0.085	0	0	0
M2_V_5%	VD model	1	1	1	1	0.141	0	0	0
M2_V_10%	VD model	1	1	1	1	0.283	0	0	0
M2_F_0.1	FD model	1	1	1	1	0	0	0.1	0
M2_F_0.3	FD model	1	1	1	1	0	0	0.3	0
M2_F_1	FD model	1	1	1	1	0	0	1	0

story by increasing stiffness, installing oil dampers, and installing friction dampers are considered in this analysis. In the models of the M2_R_1.25, 1.5 and 2, the stiffness of the first story increases by 1.25, 1.5 and 2 times compared with that of the M2. The M2_V_3%, 5% and 10% have the dashpots the viscous damping coefficients of which are calculated by $c_{d1} = 2h_d\sqrt{(m_1 + m_2)k_1}$ in the first story, where the value of h_d for each model are 0.03, 0.05 and 0.1, respectively. The M2_F_0.1, 0.3 and 1 have the EPP spring in the first story, and the yield forces are 0.1, 0.3 and 1, respectively. The yield deformation of the EPP spring is 1/360 rad in all the M2_F models.

4.2 RESULT AND DISCUSSION

4.2.1 M1 model

Figure 3 shows the resonance curve of each story of the M1 with α = 0.1, 0.2, 0.3 and 0.34. The horizontal axis of the figure is the ratio of circular frequency of excitation p to the first natural circular frequency ω_0 of the M1. As an overall feature, the value of μ_1 and μ_2 in the first mode significantly increase with increase of α, whereas those value around the second mode have little or no increase. It is seen that the value of p/ω_0 at the peak in the first mode moves to the left side, which means the model shows softening behaviour under strong excitation. This result agrees to intuitive understanding because the equivalent stiffness of the model gradually decreases with increase of the story drift as shown in the force-deformation relation in Figure 1. It is also confirmed that the jump phenomenon occurs around the fist-mode peak, which is generally seen in the non-linear system.

When the attention is focused on the result with α = 0.34, the shape of the curve around the first mode dramatically changes, and the model has more than three solutions at the same p/ω_0. It is presumed that this phenomenon is caused by the strong non-linearity in the range of large deformation; however, more investigations including the verification of stability is needed.

4.2.2 M1_R, M1_V and M1_F models

The resonance curves of the M1_R, M1_V and M1_F with α = 0.34 are displayed in Figure 4 (a), (b) and (c), respectively, in comparison with the M1. The purpose here is to clarify the effect of increasing the stiffness, installing oil dampers and installing friction dampers on the reduction in the story drift of structures.

When the stiffness increases by 1.25, 1.5 and 2 times, μ_1 and μ_2 in the first mode gradually decrease and the p/ω_0 at the peak moves to the right side, but in the second mode the maximum values of μ_1 and μ_2 are almost the same as those of the M1. Similar feature is seen in the result of the M1_F models shown in Figure 4 (c), while quite different trend can be seen in the M1_V models shown in Figure 4 (b). First of all, installing oil dampers reduce the story drift not only around the first mode but also around the second mode. Secondly, the change of the value of p/ω_0 at the peak is insignificant compared with the results of M1_R and M1_F. Thirdly, oil dampers does not work to reduce the story drift in the range of $0 \le p/\omega_0 < 0.4$ where external force act as almost static load.

In order to investigate the response characteristics of the three strengthened models, M1_R_2, M1_V_10% and M1_F_1, against large excitation, the resonance curves of these models with α = 0.68 are compared in Figure 5.

https://doi.org/10.52202/069179-0272

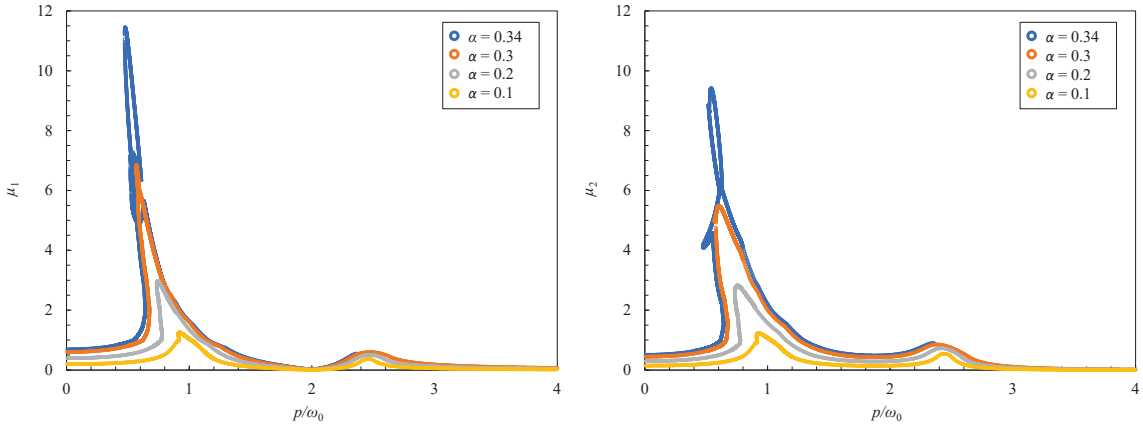

Figure 3: *Resonance curves of the M1 with α = 0.1, 0.2, 0.3 and 0.34 (left: first story, right: second story)*

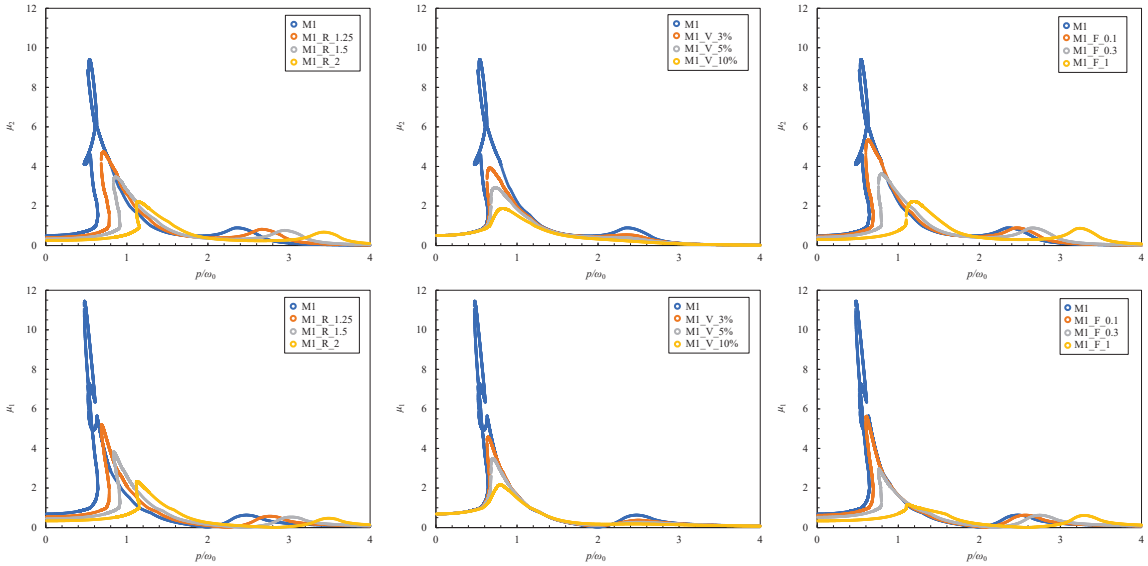

(a) M1 and M1_R_1.25, 1.5, 2 *(b) M1 and M1_V_3%, 5%, 10%* *(c) M1 and M1_F_0.1, 0.3, 1*

Figure 4: *Resonance curves of the M1, M1_R, M1_V and M1_F with α = 0.34 (top: second story, bottom: first story)*

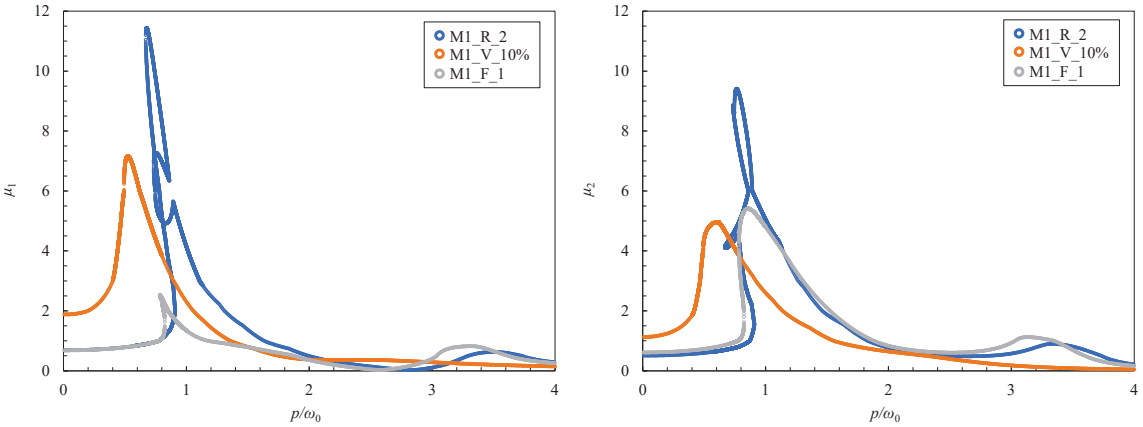

Figure 5: *Resonance curves of the M1_R_2, M1_V_10% and M1_F_1 with α = 0.68 (left: first story, right: second story)*

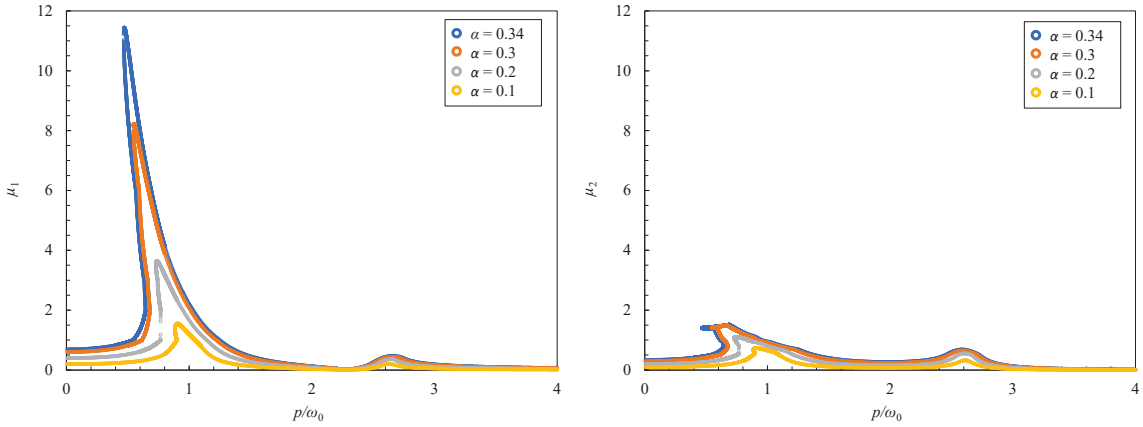

Figure 6: *Resonance curves of the M2 with α = 0.1, 0.2, 0.3 and 0.34 (left: first story, right: second story)*

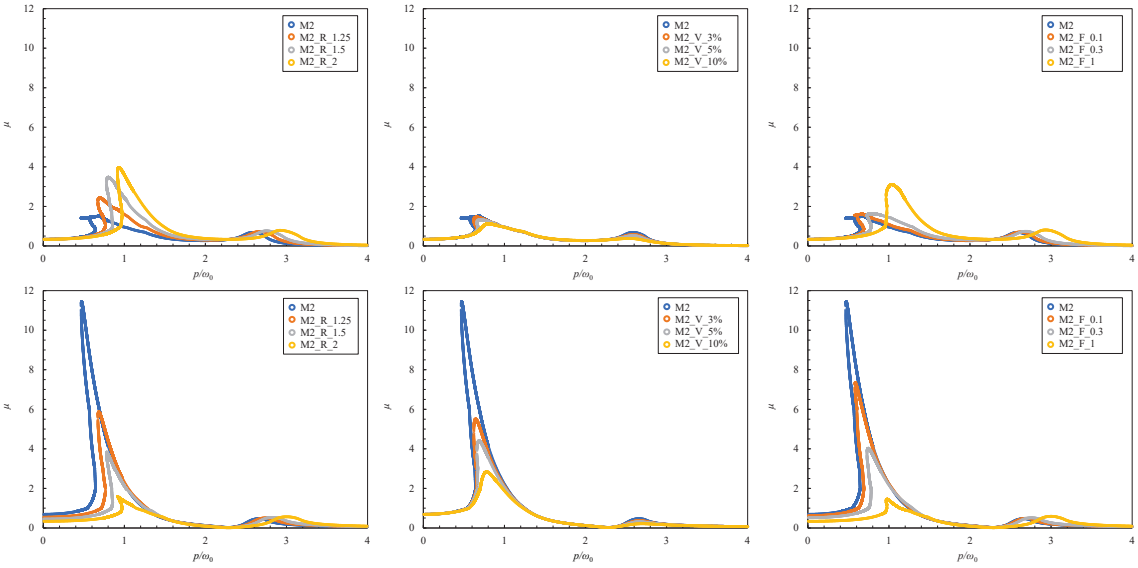

(a) M2 and M2_R_1.25, 1.5, 2 *(b) M2 and M2_V_3%, 5%, 10%* *(c) M2 and M2_F_0.1, 0.3, 1*

Figure 7: *Resonance curves of the M2, M2_R, M2_V and M2_F with α = 0.34 (top: second story, bottom: first story)*

Although these three models have similar peak values of μ_2 under the excitation with $\alpha = 0.34$, the maximum value of μ_2 of the M1_V_10% and M1_F_1 under the excitation with $\alpha = 0.68$ are smaller than that of the M1_R_2. This result indicates that the effect of strengthening by increasing stiffness, installing oil dampers and installing friction dampers highly depends on the magnitude of excitation.

4.2.3 M2 model

Figure 6 indicates the resonance curve of the M2 with α = 0.1, 0.2, 0.3 and 0.34. In this model, the story drift in the first story much larger than that of the second story especially under large excitation. This result explains the soft-story mechanism of two-story wooden houses caused by very strong earthquakes such as 1995 Kobe earthquake and 2016 Kumamoto earthquake occurred in Japan. It is also seen that the jump phenomenon occurs around the first mode and the shape is less complicated than that of the M1.

4.2.4 M2_R, M2_V and M2_F models

In Figure 7, the resonance curves of the M2_R, M2_V and M2_F are compared with that of the M2 in the same manner as Figure 4. It is seen in Figure 7 (a) that the increaseing of the stiffness of the first story decreases the story drift in the first story μ_1 but increases the story drift in the second story μ_2, indicating that when we strengthen only first story, we have to pay attention to the response of the second story even if the original structure has the relatively low stiffness and strength in the first story.

In the case of installing oil dampers or friction dampers only in the first story, the story drift in the first story gradually decreases with increase of the capacity of the dampers without significant increase of the story drift in the second story. It is presumed that the reason of this result is dut to the feature of the damper which works to

https://doi.org/10.52202/069179-0272

increase mainly damping performance not stiffness and strength.

5 CONCLUSIONS

The steady-state response of the two-degree-of-freedom-system with ENCL and EPP springs were derived and the vibration property of two-story timber structure with energy dissipation devices were discussed based on the resonance curve. The following conclusions are obtained from this study:

1. The two-degree-of-freedom-system which has ENCL springs with the parameters of timber structure shows softening behaviour and jump phenomenon around the first mode in the resonance curve.
2. The strengthening by increasing stiffness and installing friction dampers reduce the story drift only around the first mode, whereas installing oil dampers reduces the story drift both around the first and the second modes.
3. In the two-story timber structure which has relatively low stiffness in the first story, installing dampers only in first story reduces the story drift in the first story without significant increase of the story drift in the second story.

REFERENCES

[1] H. Matsunaga, Y. Miyazu, S. Soda: A Universal Modeling Method for Wooden Shear/Nonshear Walls, J. Struct. and Const. Eng., 74-639, pp. 889-896, 2009. (in Japanese)

[2] Caughey T. K.: Equivalent Linearization Techniques, Journal of the Acoustical Society of America , Vol. 35, No. 11, pp. 1706-1711, 1963

[3] Y. Miyazu: Evaluation of vibration characteristics of high-damping structure based on response curve, J. Struct. and Const. Eng., 87-798, pp. 789-798, 2022. (in Japanese)

[4] Hiroshi Tajimi: Introduction to Structural Dynamics, CORONA PUBLISHING, 1965. (in Japanese)

[5] Y. Miyazu, M. Nagano, T. Sato, M. Iguchi, T. Mikoshiba, T. Katada, K. Sugawara: Evaluation of Seismic Performance of Wooden Houses with Friction Dampers by Full-scale Shaking Table Tests, World Conference on Timber Engineering (WCTE2021), 2021.

[6] T. K. Caughey: Sinusoidal Excitation of a System With Bilinear Hysteresis, Journal of Applied Mechanics, Vol. 27, Issue 4, pp. 640-643, 1960.

[7] M. Kikuchi, K. Tamura, M. Ueda: Non-linear Steady-state Vibration of Seismically-isolated Structures with Viscously-damped Isolation System, J. Struct. and Const. Eng., 69-576, pp. 63-70, 2004. (in Japanese)